Use Of New Toughness Parameters from the Tensile Test application in characterising the Heat-affected Zone in Weld Joints

A. K. Bhaduri*, S. J. Ray* & P. Rodriguez *

A simple test procedure that can substitute the Charpy test for the estimation of ductile fracture toughness of the weakest region of a weld joint has been evolved. This approach explocits the conventional tension test with smooth round specimens, and stipulates that the post necking regime in this test is dominated by micro-void growth and coalescence processes. The method of computing two new toughness parameters from the load-elongation data of the tensile test is described. The effect of aging of the 2.25 Cr - 1 Mo steel HAZ in the Alloy 800/2.25 Cr - 1 Mo steel dissimilar metal joint (welded with inconel 182 electrodes) was studied to demonstrate the application, efficacy and sensitivity of these estimates of fracture toughness.

INTRODUCTION

The Charpy impact testing of V-notch specimens is the most popular method for characterising the toughness of weld joints. The chief attraction of this test lies in its simplicity and rapidity, and the small size of the specimen. The advent of Instrumentation in impact testing has enable a deeper probe into deformation and fracture behaviours, and has thus considerably enhanced the utility of this test 1-3. A limitation of the Charpy V test is the difficulty in evaluation toughness of weld joints at elevated service temperatures. An additional serious limitation of this test is in evaluating the minimum toughness of a weld joint. A majority of the weld joints fall in the heat-affected zone (HAZ). However, it is difficult to accurately place the notch in the weakest region of the HAZ, because : (i) the microstructure of the HAZ varies considerably across its width when it may not be possible of determine a priori which region of the HAZ has the lowest toughness ; and (ii) the weld fusion line is seldom vertical to the specimen surface. Using weld thermal simulators, it is possible to produce the HAZ microstructures; in such an approach, several specimens, each with a microstructure for a given location in the HAZ, will be required. Even then, it would be difficult to simulate the HAZ for dissimilar metal weld (DMW) joint where elemental diffusion across the weld fusion line occurs. Further, on prolonged exposure at elevated service temperatures (which can be simulated in the laboratory by giving suitable aging heat treatments), the location of the weakest region in the HAZ may change due to changes in the microstructure.

These difficulties prompted the development of a simple test procedure that can substitute the Charpy test for the estimation of ductile fracture toughness of the weakest region of a weld joint4. This procedure exploits the tension test with smooth round specimens to arrive at two estimates of fracture toughness, the r_f and n_f parameters. As this method is new, the test and computational procedures for determining these parameters from the tension test are first described, with emphasis on the physical concepts ; for mote details, Ref.4 may be consulted. Additionally, the strain localisation parameter (SLP)5, which is a measure of the extent of the contribution of nonhomogeneous plastic deformation of the micro-void growth process in the necked region, has also been computed. The emphasis in this paper is on demonstrating the application and the efficacy of the new approach in characterising the toughness of the HAZ in weld joints. The effect of aging (that simulates service exposure) the dissimilar metal weld (DMW) joint in Alloy 800/1.25 Cr - 1 Mo steel welded with Inconel 182 electrodes has been characterised using the conventional UTs and reduction in area (% RA), as well as the parameters that evolve from the new concept. In the transverse-weld specimens of this DMW joint, tensile fracture occurs in the 2.25 Ct - 1 Mo steel HAZ. The r_f and n_f evaluated on these specimens, therefore, correspond to those of the wekest region in the HAZ.

* The authors are associated with Indira Gandhi Centre for Atomic Research, Kalpakkam 603 102

FRACTURE TOUGHNESS ESTIMATE FROM TENSILE TESTS

The process of ductile fracture in smooth and notched round specimens being deformed in tension has been extensively studied 6-10. Gross micro-void nucleation, which could be determined using even an ultrasonic technique, is reported6 to occur even beyond the incipient necking point in a wide range of materials. With increasing deformation, the neck continues to develop, the mean normal stress continues to increase and microvoids continue to grow at accelerating rates to the point of incipient microvoid coalescence and the specimen ultimately fractures. In our procedure 4 it is stipulated that microvoid growth and coalescence processes dominate the post-necking regime of tensile deformation, so that energy absorbed in the specimen in this regime reflects the ductile fracture toughness.

The method of estimating toughness is described below. Figure 1 shows, a typical plot of load (P) against cross-head displacement (xt) for a tension test at constant cross-head speed carried to fracture. The specimen deforms homogeneously to the necking point (load P_n and cross-sectional area A_n).

Beyond this point, a neck developes and grows, and load decreases to P_f, the "Fracture" load beyond which the load frops "instantaneously" (i.e., within the data logging interval) to zero. It may be pointed out that this "fracture" point is better identified as the incipient micro-void coalescence point. The dashed line in Fig.1 corresponds to the theoretically computed elastic unloading line that the specimen would followed it been unloaded from the necking point. The post-necking energy of fracture W_{pn} is computed by imagining that the original specimen is unloaded from its incipient necking point to zero load (i.e., along this dashed line), and W_{pn} refers to the energy that would be consumed by this "new" specimen (with initial ununiform cross- sectional area A_n) on reloading it in tension at the same cross head speed up to fracture. W_{pn} thus equals the total area under the P-$_{xt}$ plot to the right of the loading line for this imaginary specimen (i.e. the dashed line in Fig-1). shown by the shaded area in Fig. 1. It is important to recognize that as Pf^30, at the instant of fracture the elastic energy stored in the machine (i.e., segments of the load train between the two cross-head excluding the specimen parallel length) is also spent in the fracture process, therefore, for computing E_{pn}, the cross-head displacement xk rather than specimen extension X is to be used. And this in turn leads to a great experimental simplification - it is redundant to use gauge length extensometry for the tests.

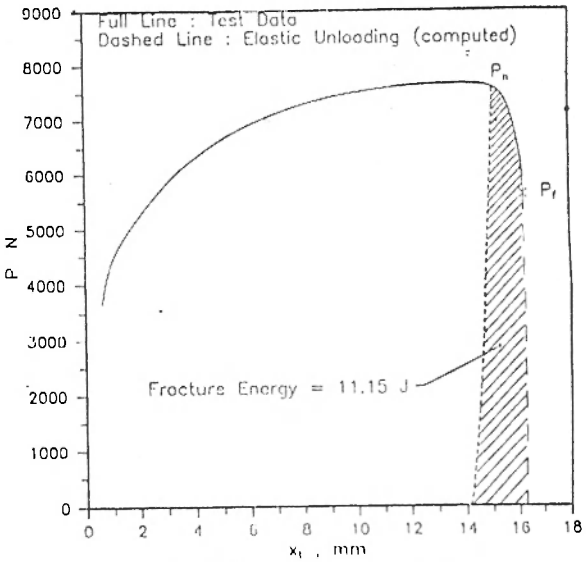

Fig. 1 : A typical P-x plot for a tensile test illustrating the concepts. The material was type 316 stainless steel (solution-annealed) tested at room temperature.

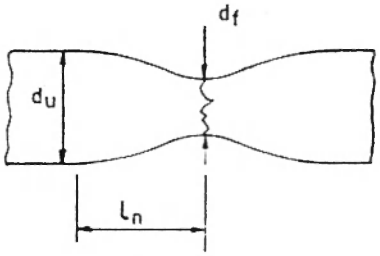

Fig. 2 : A schematic of the necked region of a tensile specimen, showing the various dimensions measured for calculating the parameter SLP.

One obvious estimate of fracture toughness is the "specific post- necking energy to fracture" $f = W_{pn}/A_n$, which measures the average energy per unit area required to cause tensile fracture. Also, if A_f is the minimum cross-sectional area at fracture, then ln (A_n/A_f) measures the average longitudinal plastic stain prependicular to the plane of the neck (ignoring the voids on this plane[8]) accumulated from the point of necking to fracture. Another estimate of toughness is the parameter $n_f = r_f / l_n (A_n/A_f)$: this parameter measure the average incremental plastic energy per unit volume consumed by the specimen per unit longitudinal plastic strain at the neck to sustain the necking i.e., fracture process.

The concept behind r_f and n_f belongs to the realm of contlnuous damage machanics approaches 6-12, the most well known of which is Kachanov's concept. In

kanchanov's concept [11,12], the decrease in effective load bearing area due to micro-voids is taken as the damage parameter. In a conventional Charpy V-notch test or a fracture mechanics test, a notch or a crack is Introduced to increase triaxiality, thereby suppressing plastic deformation and promoting fracture. The post-necking energy concept attempts to achieve the same end by discounting the energy manifestly associated with plastic deformation which can be, and usually is a very large fraction of the total energy consumed by the specimen during the entire tensile deformation to fracture. Thus r_f can be compared to Charpy V energy per unit ligament area, However, in conventional Charpy V energy per unit ligament area. However, in conventional Charpy V test with ductile specimens (i.e. in the upper shelf regime for materials undergoing duc.tile to brittle transition) considerable energy is absorbed in plastic deformation ; therefore r_f should reflect the fracture toughness (i.e. energy for ductile fracture process) much better than does the Charpoy V energy. On the other hand, unlike in fracture machanics tests employing specimens containing sharp cracks r_f and n_f eatimate fracture toughness not for the virgin material or for material at low plastic deformation level, but after the material has undergone extensive plastic straining and consequent work hardening.

As tensile test are most extensively used to characterise the plastic deformation properties of weld joints at desired temperature, the advantages of being able to arrive at estimates of fracture toughness from the same test are obvious. Applied to a transverse - weld tensile specimen the most consenative toughness property for the weld joint is automatically evaluated by this method, as failure occurs in the weakest region of the specimen. So far as the testing paraphernallia is concerned, as already Indicated gauge length extensometry is not necessary, Similarly, testing temperature should also not pose any limitations.

EXPERIMENTAL

Materials for Testing

Single V-groove butt joints, with an included angle of 80°, were prepared between 12 mm thick plates of solution annealed Alloy 800 and normalised and temperaed 2.25 Cr - 1 Mo steel, and welded using Inconel 82/182 consumables.The plates were set up in the flat (1G) position and welded using the tungsten inert gas (TIG) process for the first two root passes and the manual metal arc (MMA) process for the subsequent passes. The chemical compositions of the weld and base metals are given in Table 1, and the welding conditions used are given in Table 2. The details of the weld joint design and the non-destructive test carried out have been reported13,14 elsewhere.

Table 1 : Chemical composition of materials used. Wl-%

Element	Alloy 800	Inconel 182	2.25Cr-1Mo Steel
C	0.033	0.05	0.06
Si	0.27	0.56	0.18
Mn	0.86	7.84	0.47
P	0.009	0.01	0.47
S	0.009	0.004	0.008
Cr	19.5	13.8	0.008
Ni	30.8	66.2	2.18
Mo	0.10	-	-
Al	0.14	-	0.93
Ti	0.39	0.40	-
Nb	0.017	1.84	-
V	0.05	-	0.01
Cu	0.05	-	-
Co	0.22	-	-
Fe	Balance	7.58	Balance

Based on a detailed evaluation of the conventional tensile properties of this DMW joint, its optimum post-weld heat treatment (PWHT) temperature was found to be 973 K[14,15]. Hence, in this investigation, this joint was subjected to a 1h PWHT at 973k and subsequently aged at 873 K for 0,100,500,1000 and 5000 h. To prepare the tensile specimens the root region of the weld pads were first completely machined off to ensure that the weld metal consisted entirely of the MMA deposit. Button-head type transverse-weld tensile test specimens, with circular cross- sections and with 26.3 mm paralles length and 4 mm guage diameter, were then machined from these weld pads.

Table 2 : Welding conditions used

	1st two Root Phases	Subsequent Passes
Welding Process	TIG	MMAW
Welding consumable	Inconel 82	Inconel 182
Consumable specification	ERNiCr-3 (AWS 5,14)	ENiCrFe-3 (AWS 5,1)
Consumable diameter (nm)	1.6	2.4
Polarity	DCEN	DCEP
Welding current (Amps.)	70	50-75
Preheat temperature (K)	473-523	473-523

Tensile Testing : Data Acquisition

The tension tests were carried out at room temperature (RT = 300 K) in a screw-driven floor model INSTRON 1195 machine at a constant cross-head speed of 0.5 mm. min-1 without using any extensometers. In this Investigation one sample each was tested for each ageing condition, as execellent repeatability of the results had been established in our previous study[4]. The values for the initial specimen parallel length and cross-sectional area, L_o and A_o respectively, were accurately determined prior to testing. The ten-step load suppression unit of INSTRON was used to enhanced load resolution. The load-time (P-t) data were acquired in a 8088/8089--based personal computer using a 5 1/2- digit digital voltmeter through an IEEE-488 interface, with an appropriate software in complied Basic. The time interval between successive load data was about 0.11 s, and the effective load resolution was about 2×10^{-5}.

Tensile test Data Analysis

The P-t data generated were analysed using a 80386/80387- based personal computer with appropriate softwares written in the C- language. The details of the calibration procedure and computational method will be found in the previous report4, and the relevant equations will be found in Ref. 16. The data analysis procedure consists of the following steps.

First from the P-t data, the cross-head displacement (x_t) and specimen extension (x) values were calculated using the theoretically computed specimen elastic compliance (Csp) and the experimentally determined[4] machine elastic compliance. (C_m) values. Secondly, the necking point (load P_n in Fig. 1) was graphically identified as the point where din P/dx = -1 (Lo + x). As the specimen deformation is homogeneous up to this point, in this regime $L_oA_o = L_k = L_nA_n$, where L and A are instantaneous values of parallel length and cross-sectional area of specimen, and l_n A_n the corresponding values at necking point. This property is invoked to compute An Next, the elastic unloading line (Dashed line in Fig 1.) was computed using the theoretically computed value of C_{sp} at the necking point (load P_n) and the experimentally determined Cm-P relation. The post-necking energy W_{pn}/A_n and n_f = r1n (A_n/A_f) were calculated.

It is obvious from Fig. 1 that the two key requirements for accurately determining of W_{pn} are : (i) accurately determining the point of specimen necking; and (ii) having sufficient data resolution P-t data during the tension test.

Other Tensile Property Parameters

The other conventional tensile property parameters that were determined from the $P-x_t$ plot are the ultimate tensile strength (UTS) and the, reduction in area RA = $(a_o-A_f)/A_o$. Also, as the "necking" and "fracture" points on the $P-x_t$ plots could be accurately identified, additional parameters such as the true necking stress $\delta n = P_n/A_n$, reduction in area from the necking point RA_n = $(A_n - A_f) / A_n)$, and the fracture stress $\delta f = P_f / A_o$ were determined.

The strain localisation parameter (SLP) was measured by projecting the profile of the fractured specimens, and at the fractured end of the neck d_f, as well as the average length of the neck from its base to its fractured end (l_n). as shown schematically in Fig. 2. The strain localisation parameter (SLP) is defined as : SLP = $(d_u-d_f) /l_n$.

RESULTS AND DISCUSSION

Figure 3 shows the variation in the different strength parameters with ageing duration at 873 K. The values of δn values. The variations in all these three strength parameters with duration of aging at 873 K were similar; the strength values initially decreased slightly, showing weak minima after 500 h of again, and then remained practically unchanged beyond 100h of aging. It is interesting to note, however the extent of variation in both s_n and s_f values with aging time where more than that for UTS; indeed, the variation in UTS was within = 3%, the typical scatter band for UTS. As expected, the values of % RA_n were lower than those for the conventional ductility parameter % RA (fig. 4) the variation in these parameters with ageing time were similar - initial increase leading to maxima after 1000h of aging beyond which they decreased quite sharply. However, % RA varied within a range of = 3% (the typical scatter band) while the variation in %RA_n with ageing duration was somewhat more pronounced. It is Interesting to note from Figs 3 & 4, that the minima in the strength parameters (occurring after 500h of aging) do not coincide with the maxima in the ductility parameters (occuring after 1000h of aging). For optimising toughness, even intuitively it can be seen that it is necessary to adopt a single parameter that would combine both strength

and ductility, the energy - based parameters being the obvious choice.

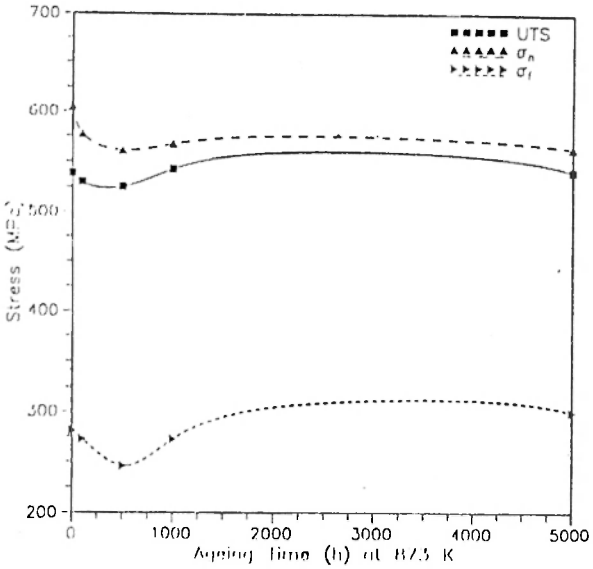

Fig. 3 : Variation in UTS, σ_n and σ_f at room temperature with duration of aging.

Figure 5 shows the effect of duration of aging on the two new toughness parameters, viz r_f and n_f, r_f shows a prominent maximum after 500h of aging , while nf seems to indicate a saturation after 100 h of aging. The dip in n_f for 1000h of aging could be due to data scatter. On the other hand it could reflect14 a complex interplay between precipitate coarsening and carbon migration from HAZ to weld metal, which progresses with different kinetics.

Figure 6 depicts the percent changes in r_f, n_f, UTS and %RA with ageing time compared to unaged (i.e. aging time - 0) condition. As already noted, the range of variations in them UTS and %RA are within + 2-3%, the typical scatter band for these parameters. Thus aging at 837 K up to 5000 h has no detectable effect on these properties for this joint subjected to PWHT at 973 K. On the other hand, the parameters r_f and n_f showed variations in the range of 7 ro 18% on aging at 873 in the toughness of 2.25 Cr - 1 Mo steel HAZ (where tensile failure occurs). This clearly demonstrates both the efficacy and the sensitiveness of the new toughness parameters, as also their usefulness in characterising the toughness of weld joints.

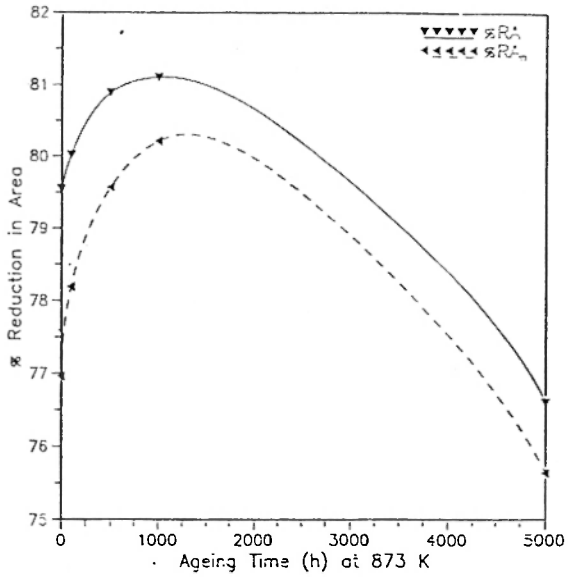

Fig. 4 : Variation in % RA and %RA_n at room temperature with duration of aging.

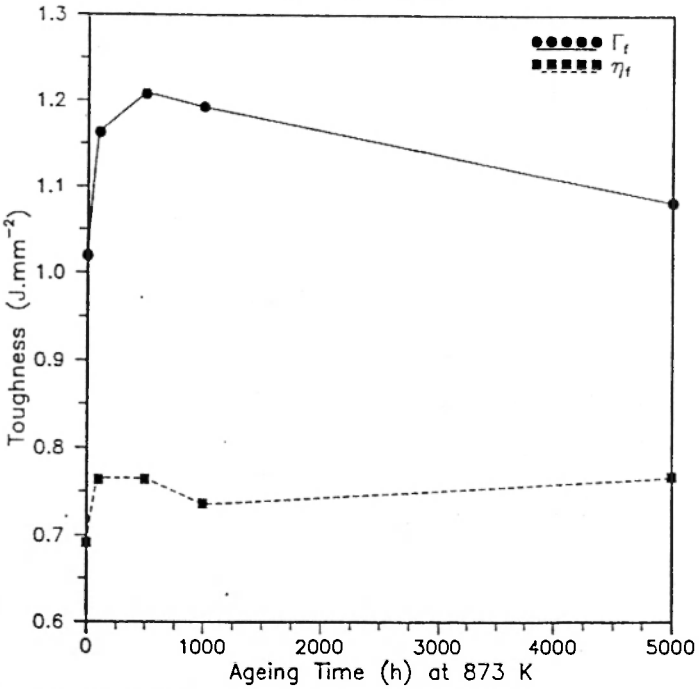

Fig. 5 : Variation in n_f and n_f at room temperature with duration of aging.

As shown in Fig. 7, the strain localization parameters SLP initially increased with aging time to its maximum value after 500 h of aging, beyond which it decreased quite steeply, the variation in SLP with the duration of aging showed essentially the same trend as that of r_f (Fig.5), with the aging time for the peak in SLP coinciding with the minima in the strength parameters. This is to be expected micro-void growth is controlled by plasticity, in this case higher the strain localisation

at the neck (i.e. higher the SLP), higher would be the energy required for the non-homogeneous plastic deformation of the neck, and thus r_f. Further, the value of SLP changed in the range of + 7% to 18% with duration of ageing at 873 K. Clearly, therefore SLP is another sensitivity parameter for characterising the changes in the weakest region of the weld joint, which in this particular case is the 2.25 Cr - 1 Mo steel HAZ.

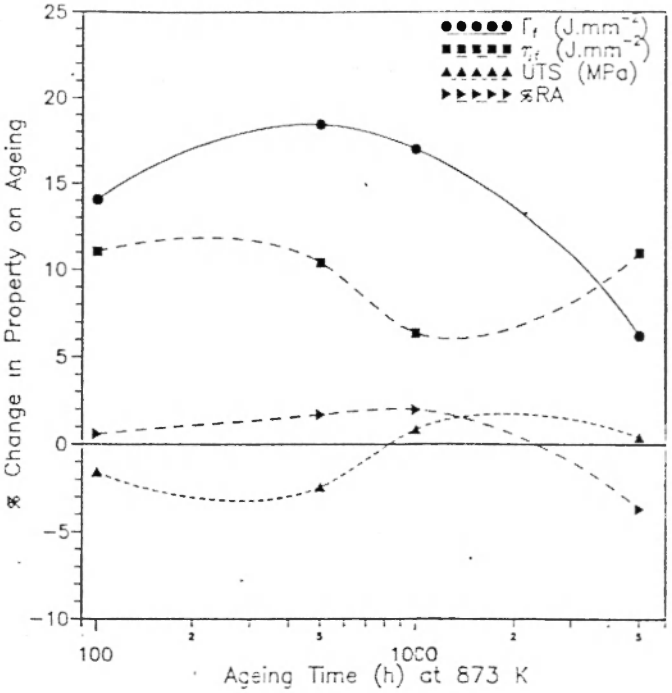

Fig. 6 : Comparison of the sensitivity of toughness parameters, η_f and η_τ, and the conventional tensile property parameters at room temperature on aging.

CONCLUSION

The testmethod evolved for estimating the new toughness parameters from the tensile test by measuring r_f and n_f is attractive for a rapid estimation of fracture toughness, particularly for applications like potimising PWHT for weld joints. Compared to the conventional strength and ductility parameters determined from tension tests, r_f and n_f were found to be more sensitive to the effect of aging for the 2.25 Cr - 1Mo steel HAZ in the Alloy 800/2.25 Cr - 1 Mo steel DMW joint. An attractive feature of this test method, it bears stressing, is that the regular tensile test to fracture of this test method, it bears stressing, is that the regular tensile test to fracture is adquate to yield these toughness parameters. The other parameters, namely of δ_n and % RA_n and SLP, were also more sensitive to the effects of aging than the conventional strength and ductility parameters, viz. UTS and %RA.

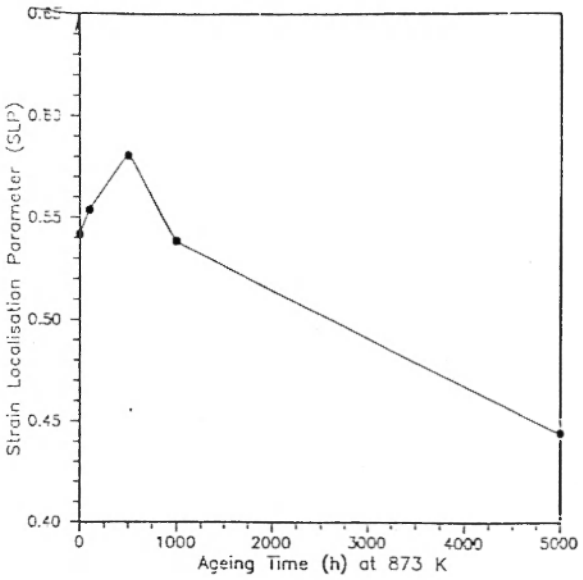

Fig 7 : Variation in SLP at room temperature with duration of aging.

REFERENCES

1. K. G. Samuel, P. R. Sreenivasan, S. K. Ray and P. Rodriguez, J. Nucl. Mater. 150 (1987) 78.
2. S. K. Ray, P. R. Sreenivasan, K. G. Samuel and P. Rodriguez, Int. J. Pres. Vessel & Piping (1992) in press.
3. P. Rodriguez, S. L. Mannan and S. K. Ray, in Advances in Structural Testing, Analysis and Design, Tata Mc Graw-Hill Publ. Co. Ltd., Bangalore (1990) p. 1037.
4. S. K.Ray, A. K. Bhaduri and P. Rodriguez, communicated to J. Nucl. mater.
5. S. K. Ray, A. K. Bhaduri and P. Rodriguez, to be published.
6. J. I. Bluhm and R. J. Morrisy, Proc. Int. Conf. on Fracture, Japan Inst. Metals, Sendai (1965) p. 1737.
7. V. Tvergaard and A. Needleman, Acta Metall. 32 (1984) 157.
8. P. F. Thomson, in Ductile fracture of Metals, Pergamon Press, Oxford (1990) ch. 6.
9. M. Zheng, Z. J. Luo and X. Zheng, ENGG. FRACT. MECH. 41 (1992) 103.
10. K. S. Zheng and C. Q. Zheng, Eng. mech. 39 (1991) 851.
11. L. M. Kachanov, in Introduction to Continuus Damage Mechanics, Martinus Nijhoff, Dordricht (1990) ch. 1.
12. Jean Lemaitre and Jean-Louis Chabioche, In Machanics of Solid materials, Cambridge University Press Cambridge (1990) ch.7.
13. A. K. Bhaduri, Metallurgical Studies for the Development, Characterisation and Evaluation of an Improved Transition Metal Joint Steam Generators, Ph. D. Thesis, Ind. Inst. Techno., Kharagpur (1990).
15. A. K. Bhaduri, S. Venkadesan, P. Rodriguez and P. G. Mukunda, mater. Sci. Technol. 7 (1991) 1051.
16. S. K. Ray, p. Rodrigeunez and D.H.Sastry, communicated to Trans, Ind. Inst. metals.